JOURNAL OF AIRCRAFT
Vol. 45, No. 2, March–April 2008

Engineering Notes

ENGINEERING NOTES are short manuscripts describing new developments or important results of a preliminary nature. These Notes should not exceed 2500 words (where a figure or table counts as 200 words). Following informal review by the Editors, they may be published within a few months of the date of receipt. Style requirements are the same as for regular contributions (see inside back cover).

Effect of $C_{\varepsilon 1}$ on the Performance of the Menter One-Equation Model of Turbulence

M. Elkhoury*
Lebanese American University, Byblos, Lebanon

DOI: 10.2514/1.34567

Introduction

ONE-EQUATION models of turbulence are widely used in aeronautical applications, mainly due to their simplicity, low computational cost compared with higher-order models, and good level of accuracy in external aerodynamic flows. These models have different origins: Baldwin and Barth [1] (BB) derived their model from the transformation of the k-ε model with some additional assumptions. Spalart and Allmaras [2] (SA) developed their model based on the arguments deduced from dimensional analysis. Menter [3] established a clear and firm connection between one- and two-equation models of turbulence. Goldberg [4,5] proposed a model with terms similar to those of Baldwin and Barth [1] in the high-Reynolds-number form and suggested a treatment to the destruction term near shear-layer edges. Nagano et al. [6] derived their one-equation model from a low-Reynolds-number k-ε closure, which resulted in many damping functions. Their model showed very good results when compared with direct numerical simulation and experimental data for wall-bounded flows. Fares and Schroder [7] transformed the Wilcox k-ω closure [8] to a one-equation model based on Menter's [3] approach and applied it to free-shear and wall-bounded flows. Elkhoury [9] proposed some modifications to Menter's model and tested the effects of the destruction term that resulted from the transformation of the k-ω equation on the predictive capabilities of the model.

The Menter model's constants are based on the standard values of the k-ε model. The criteria that were used to determine these constants are based on simple flow cases: $c_{\varepsilon 2}$ is determined using the decay of isotropic turbulence, $c_{\varepsilon 1}$ followed from the formulation of the transport equations for k and ε assuming homogeneous shear flow, and σ_k is determined using an oscillating-grid turbulence for which the mean flow has a zero velocity (both convective and production terms are zero). The relationship between the constants σ_ε, c_μ, $c_{\varepsilon 1}$, and $c_{\varepsilon 2}$ is determined using the slope of the mean-velocity profile in logarithmic layers. These coefficients are held constant when the model is applied to different geometries and Reynolds numbers. However, several studies [10–13] based on the Reynolds stress turbulence models concluded that these coefficients should be a function of flow parameters. To account for the effect of near-wall anisotropy, researchers [14–16] have introduced a variable $c_{\varepsilon 1}$, depending on various geometries and flow parameters. Durbin [11] used the distance from the wall and Shih et al. [12] formulated an equation for $c_{\varepsilon 1}$ that is based on the production-to-dissipation ratio. Yakhot and Orszag [13] used the ratio of the turbulent to mean-strain time scale in the formulation of $c_{\varepsilon 1}$.

In line with the preceding research, the present work modifies the Menter model by introducing a variable $c_{\varepsilon 1}$ in front of the production and destruction terms. This modification follows from the k-ε turbulence closure for which the coefficient $c_{\varepsilon 1}$ is a function of flow parameters. The validity of the model incorporating the present modification is tested in adverse-pressure-gradient, shock/boundary-layer interaction, and the computed results are assessed against the original Menter model, the Spalart–Allmaras model, and experiments.

Menter One-Equation Model of Turbulence with Variable $C_{\varepsilon 1}$ Coefficient

The derivation of the single-equation model starts by transforming the high-Reynolds-number form of the following standard two-equation k-ε turbulence model:

$$\frac{Dk}{Dt} = \tilde{\nu}_T\left(\frac{\partial u}{\partial y}\right)^2 + \frac{\partial}{\partial y}\left(\frac{\tilde{\nu}_T}{\sigma_k}\frac{\partial k}{\partial y}\right) - \varepsilon$$
$$\frac{D\varepsilon}{Dt} = c_{\varepsilon 1}\frac{\varepsilon}{k}\tilde{\nu}_T\left(\frac{\partial u}{\partial y}\right)^2 + \frac{\partial}{\partial y}\left(\frac{\tilde{\nu}_T}{\sigma_\varepsilon}\frac{\partial \varepsilon}{\partial y}\right) - c_{\varepsilon 2}\frac{\varepsilon^2}{k} \tag{1}$$

where $D()/Dt$ denotes the substantial derivative. The substantial derivative of the eddy viscosity $\tilde{\nu}_T = c_\mu(k^2/\varepsilon)$ becomes

$$\frac{D\tilde{\nu}_T}{Dt} = 2\frac{\tilde{\nu}_T}{k}\frac{Dk}{Dt} - \frac{\tilde{\nu}_T}{\varepsilon}\frac{D\varepsilon}{Dt} \tag{2}$$

After substituting Eq. (1) into Eq. (2), two assumptions are used to eliminate the dependency on k and ε in Eq. (2). The first is by assuming that the Bradshaw relation is valid; that is, the turbulent shear stress is proportional to the turbulent kinetic energy:

$$|-\bar{u}\,\bar{v}| = \sqrt{C_\mu}k = \tilde{\nu}_T\left|\frac{\partial u}{\partial y}\right|$$

The second follows by assuming that the diffusion coefficients in the k and the ε equations are identical. The resulting high-Reynolds-number single-equation model follows as

$$\frac{D\tilde{\nu}_T}{Dt} = ((c_{\varepsilon 2} - c_{\varepsilon 1})\sqrt{c_\mu})\tilde{\nu}_T\left|\frac{\partial u}{\partial y}\right| + \frac{\partial}{\partial y}\left(\frac{\tilde{\nu}_T}{\sigma}\frac{\partial \tilde{\nu}_T}{\partial y}\right)$$
$$-\left(\frac{(c_{\varepsilon 2} - c_{\varepsilon 1})\sqrt{c_\mu}}{\kappa^2} + \frac{1}{\sigma}\right)\frac{\tilde{\nu}_T^2}{L_{\mathrm{VK}}^2} \tag{3}$$

where L_{VK} is the von Kármán length, defined as

$$\frac{1}{L_{\mathrm{VK}}^2} \rightarrow \frac{\frac{\partial \Omega}{\partial x_j}\frac{\partial \Omega}{\partial x_j}}{\Omega^2}$$

The detailed derivation of Eq. (3) can be found in [3]. The low-Reynolds-number general form of Eq. (3) becomes

Received 13 September 2007; revision received 12 November 2007; accepted for publication 18 November 2007.

*Assistant Professor, Department of Mechanical Engineering, P.O. Box 36; mkhoury@lau.edu.lb.

$$\frac{D\tilde{\nu}_T}{Dt} = ((c_{\varepsilon 2} - c_{\varepsilon 1})\sqrt{c_\mu})D_1\tilde{\nu}_T\Omega + \frac{\partial}{\partial x_j}\left(\frac{\tilde{\nu}_T}{\sigma}\frac{\partial\tilde{\nu}_T}{\partial x_j}\right) - \left(\frac{(c_{\varepsilon 2} - c_{\varepsilon 1})\sqrt{c_\mu}}{\kappa^2} + \frac{1}{\sigma}\right)\min\left(\frac{\tilde{\nu}_T^2}{L_{\text{VK}}^2}, \frac{\Omega\tilde{\nu}_T^2\sqrt{\tilde{\nu}_T/\nu}}{\nu}\right) \quad (4)$$

With the following damping function introduced in front of the production term [3], $D_1 = (\nu_T + \nu)/(\tilde{\nu}_T + \nu)$. The damped eddy viscosity is computed using

$$\nu_T = \tilde{\nu}_T D_2 \quad \text{with} \quad D_2 = 1 - e^{-(\tilde{\nu}_T/A^+\kappa\nu)^2} \quad (5)$$

Here, Ω is the absolute value of the vorticity. The standard k-ε model's constants that are used in Eq. (4) are $c_{\varepsilon 1} = 1.44$, $c_{\varepsilon 2} = 1.92$, $\sigma = \sigma_k = 1.0$, and $c_\mu = 0.09$, with the von Kármán constant $\kappa = 0.41$. The coefficient A^+ is set equal to 13.0.

In the derivation of $c_{\varepsilon 1}$ using the k-ε model for homogeneous shear flow, one arrives at $c_{\varepsilon 1} = 1.0 + \varepsilon/P_k(c_{\varepsilon 2} - 1.0)$. This clearly demonstrates the dependency of $c_{\varepsilon 1}$ on the ε/P_k, which motivates a modification that includes the destruction-to-production ratio. The value of $c_{\varepsilon 1} = 1.44$, popular in use, corresponds to $\varepsilon/P_k \sim 0.48$. In nonequilibrium adverse-pressure-gradient flows, the production/destruction ratio can considerably exceed one, resulting in excess shear stress prediction. To limit this effect for the present model, a proposed variable such as $c_{\varepsilon 1} \propto 1.44/(\text{destruction/production})$ was adopted. Unlike the original formulation [3], this variable function for $c_{\varepsilon 1}$ influences both the destruction and the production terms in the present formulation. One eligible function that satisfies this behavior may be written as

$$c_{\varepsilon 1} = 1.44/\min(1.0, \max(r^n, C_{\min})) \quad (6)$$

where

$$r \equiv \frac{\tilde{\nu}_T}{\Omega\kappa^2 L_{\text{VK}}^2}$$

is the destruction-to-production ratio of the present model. The shear stress varies as $|-\bar{u}\,\bar{v}| \propto (\text{production/destruction})^n k$ with $n = 0.5$ for two-equation models and $n = 0$ for Bradshaw's relation, encouraging the usage of the power n in Eq. (6). Using the limiter of Eq. (6) allows for a variation of $c_{\varepsilon 1}$ between a minimum of 1.44 and a maximum value determined by $1.44/C_{\min}$. After experimenting with several nonequilibrium-flow test cases, some of which are reported herein, the values of n and $C_{\min}$ are set to 0.01 and 0.8, respectively. Although $c_{\varepsilon 1}$ ranges between 1.44 and 1.8, it hardly exceeds a value greater than 1.6 in the outer part of the boundary layer for all considered test cases. It is worth mentioning that with the preceding modification, Eq. (4) is solved as is (that is, with the following destruction term):

$$\min\left(\frac{\tilde{\nu}_T^2}{L_{\text{VK}}^2}, \frac{\Omega\tilde{\nu}_T^2\sqrt{\tilde{\nu}_T/\nu}}{\nu}\right)$$

The destruction term of the original Menter model used for comparison is herein taken as

$$7\ \min\left(\frac{\tilde{\nu}_T^2}{7L_{\text{VK}}^2}, \frac{\partial\tilde{\nu}_T}{\partial x_j}\frac{\partial\tilde{\nu}_T}{\partial x_j}\right)$$

as suggested in [9]. This limiter (to avoid singularity when $L_{\text{VK}}^2 \to 0$) seems to have some influence on the solution, especially in shock/boundary-layer interaction flows, whereas the limiter used in the present study is

$$\frac{\Omega\tilde{\nu}_T^2\sqrt{\tilde{\nu}_T/\nu}}{\nu} \gg \frac{\tilde{\nu}_T^2}{L_{\text{VK}}^2}$$

and the original formulation is always recovered.

Numerical Method and Validation Test Cases

An implicit, thin-layer, time-dependent, compressible or incompressible Navier–Stokes solver was employed. The solver features a third-order-accurate Osher's upwind-biased flux-difference-splitting scheme. The viscous fluxes are computed with

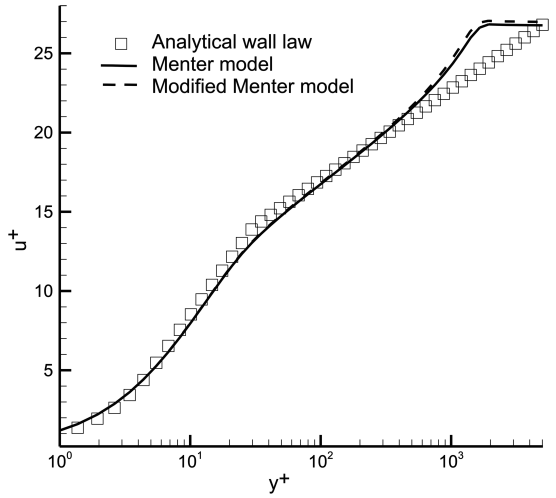

Fig. 1 Comparison of numerical and analytical wall-law profiles for a flat plate with a zero pressure gradient at 60% of the chord.

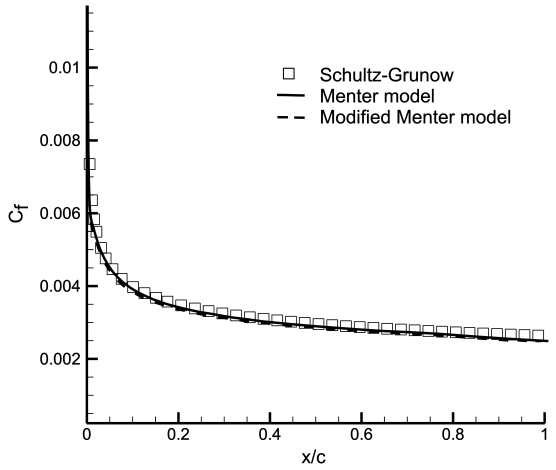

Fig. 2 Comparison of numerical and empirical skin-friction profiles for a flat plate with a zero pressure gradient.

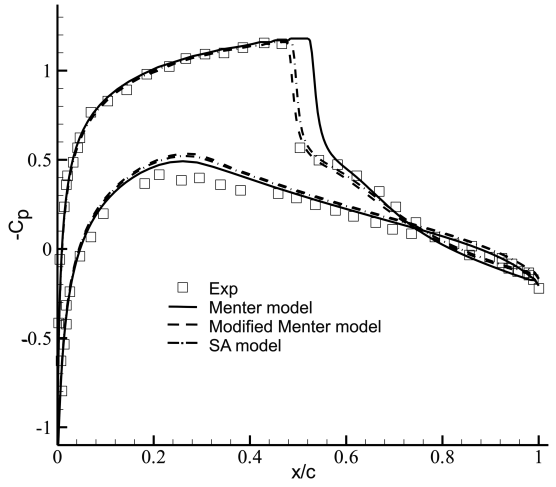

Fig. 3 Computed and measured pressure coefficient distribution of the NACA 0012 airfoil.

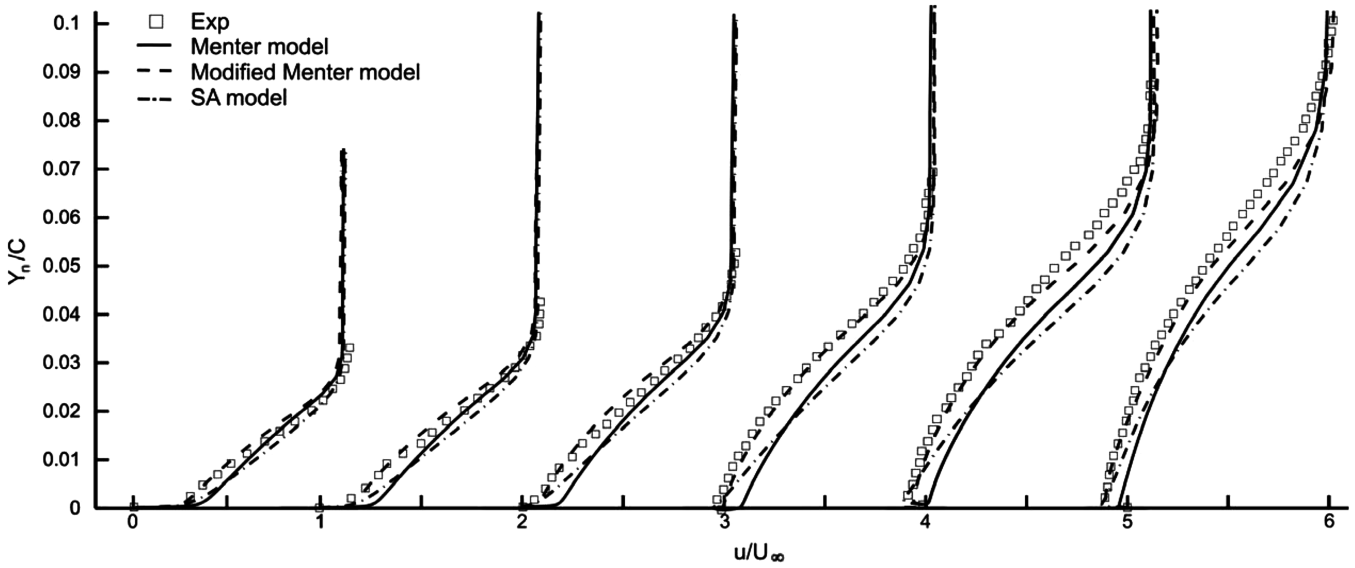

Fig. 4 Computed and measured mean streamwise velocity profiles for the NACA 4412 airfoil at $x/c = 0.675, 0.731, 0.786, 0.842, 0.897$, and 0.953 on the suction surface of the airfoil.

second-order-accurate central differences. The present model is solved and decoupled using an implicit approximate factorization method. Further details regarding the numerical implementation are available in [17,18].

Flow over a Flat Plate at Zero Pressure Gradient

This case is considered in this study to demonstrate that the present modification has no effect for equilibrium flows. The freestream Mach number was set to 0.3 and the Reynolds number was taken as 6.0×10^6. The flow was computed on an 81×81 grid with the first point off the wall yielding a y^+ value around 0.5. Comparison of the Menter model with and without the present modification is made with analytical wall-law profile and is given in Fig. 1. The computational profile was taken at 60% of the plate. In the viscous sublayer, buffer, and logarithmic layers, results are indistinguishable and collapse very closely on the analytical solution. The skin friction is plotted along the flat plate in Fig. 2. The turbulence model with and without the proposed modification is compared with the empirical Schultz–Grunow correlation described in [19] $C_f/2 = 0.185/(\log_{10}\Re_x)^{2.584}$. The skin-friction profiles predicted by the original and the modified Menter models overlap and show good agreement with the profile predicted by the Schultz–Grunow correlation.

Flow over a NACA 0012 Airfoil

This is one of the most challenging test cases due to the marked sensitivity of turbulence models predicting flows with shock-induced separation. The angle of attack of the airfoil was set to 2.26 deg with a Reynolds number of 9.0×10^6 and a Mach number of 0.799. A 257×69 grid was adopted, with 223 points lying on the airfoil surface and an extending far field to approximately 23 chords. Comparisons of the surface pressure coefficient with the experiments [20] are depicted in Fig. 3. The modified Menter model shows remarkable improvement over both the original Menter and the Spalart–Allmaras models by more precisely predicting the location of the shock.

Flow over a NACA 4412 Airfoil

This last test case is considered to ascertain the ability of the modified model to reproduce the experimental velocity profiles by Coles and Wadcock [21]. The flow over the airfoil was computed at an angle of attack of 13.87 deg, a Reynolds number of 1.52×10^6, and a Mach number of 0.2. A 257×91 grid was used, with 191 nodes lying on the airfoil surface with a far field set approximately at 22 chords. The boundary layer was artificially tripped in the present computation (for both the modified and the original Menter models) at 2.5 and 10.3% of the chord on the upper and lower surfaces of the airfoil, respectively. The SA model was run accompanied by its transition terms. Transition location is extremely important because it has a direct influence on the computed velocity profiles. Researchers tend to run this and other test cases (such as the Aerospatiale A airfoil) fully turbulent, in an attempt to alleviate the difference between the computed and measured velocity profiles. Figure 4 compares the computed mean-velocity profiles of the Menter model with and without the modification, the SA model at several stations on the upper surface of the airfoil, and experimental measurements. Predictions with the present modification clearly outperform both the original Menter and the SA models. The Menter model with the present modification accurately accounts for the nonequilibrium effect by correctly reproducing the separation-bubble height.

Conclusions

A variable coefficient ahead of both the production and destruction terms was successfully implemented into the Menter model. This modification is in line with the two-equation k-ε models that use a variable $c_{\varepsilon 1}$. The variable coefficient has no effect on equilibrium flows and was optimized for several external aerodynamic flows, two of which were considered herein. The findings show that the Menter model with the present modification has a good predictive accuracy in complex aerodynamic flows. However, this does not justify the general applicability to the higher complexity of anisotropic and nonequilibrium turbulence that occurs in many other practical flows. The source of concern arises as to whether the von Kármán length scale associated with the variable $c_{\varepsilon 1}$ is sufficient for describing more complex three-dimensional flowfields.

References

[1] Baldwin, B., and Barth, T., "A One-Equation Turbulent Transport Model for High Reynolds Number Wall-Bounded Flows," NASA TM 102847, 1990.

[2] Spalart, P., and Allmaras, S., "A One-Equation Turbulence Model for Aerodynamic Flows," AIAA Paper 92-0439, 1992.

[3] Menter, F. R., "Eddy Viscosity Transport Equations and Their Relation to the k-ε Model," *Journal of Fluids Engineering*, Vol. 119, No. 4, 1997, pp. 876–884.

[4] Goldberg, U., "Hypersonic Flow Heat Transfer Prediction Using Single Equation Turbulence Models," *Journal of Heat Transfer*, Vol. 123, No. 1, 2001, pp. 65–69. doi:10.1115/1.1337653

[5] Goldberg, U., "Turbulence Closure with a Topography-Parameter-Free Single Equation Model," *International Journal of Computational Fluid Dynamics*, Vol. 17, No. 1, 2003, pp. 27–38. doi:10.1080/1061856031000083459

[6] Nagano, C., Pei, C., and Hattori, H., "A New Low-Reynolds-Number One-Equation Model of Turbulence," *Flow, Turbulence and Combustion*, Vol. 63, Nos. 1–4, 2000, pp. 135–151. doi:10.1023/A:1009924002401

[7] Fares, E., and Schroder, W., "A General One-Equation Turbulence Model for Free Shear and Wall-Bounded Flows," *Flow, Turbulence and Combustion*, Vol. 73, Nos. 3–4, 2005, pp. 187–215. doi:10.1007/s10494-005-8625-y

[8] Wilcox, D. C., *Turbulence Modeling for CFD*, 2nd ed., DCW Industries Inc., La Cañada, A, 2000.

[9] Elkhoury, M., "Assessment and Modification of One-Equation Models of Turbulence for Wall-Bounded Flows," *Journal of Fluids Engineering*, Vol. 129, No. 7, 2007, pp. 921–928. doi:10.1115/1.2743666

[10] Lumley, J. L., "Computational Modeling of Turbulent Flows," *Advances in Applied Mechanics*, Vol. 18, 1978, pp. 123–177.

[11] Durbin, P. A., "Near-Wall Turbulence Closure Modeling Without Damping Functions," *Theoretical and Computational Fluid Dynamics*, Vol. 3, No. 1, 1991, pp. 1–11.

[12] Shih, T. H., Liou, W. W., Shabbir, A., Yang, Z., and Zhu, J., "A New k-ε Eddy Viscosity Model for High Reynolds Number Turbulent Flows," *Computers and Fluids*, Vol. 24, No. 3, 1995, pp. 227–238. doi:10.1016/0045-7930(94)00032-T

[13] Yakhot, V., and Orszag, S., "Renormalization Group Analysis of Turbulence," *Journal of Scientific Computing*, Vol. 1, No. 1, 1986, pp. 3–51. doi:10.1007/BF01061452

[14] Reynolds, W. C., "Fundamentals of Turbulence for Turbulence Modeling and Simulation," Von Kármán Inst. Lecture Series, AGARD Rept. 755, 1987.

[15] Ristorcelli, J. R., Lumley, J. L., and Abid, R., "A Rapid-Pressure Covariance Representation Consistent with the Taylor-Proudman Theorem Materially-Frame-Indifferent in the 2D Limit," *J. Fluid Mech.*, Vol. 292, 1995, pp. 111–152.

[16] Girimaji, S. S., "Pressure-Strain Correlation Modeling of Complex Turbulent Flows," *Journal of Fluid Mechanics*, Vol. 422, No. 1, 2000, pp. 91–123. doi:10.1017/S0022112000001336

[17] Ekaterinaris, J. A., Cricelli, A., and Platzer, M. F., "A Zonal Method for Unsteady Viscous, Compressible Airfoil Flows," *Journal of Fluids and Structures*, Vol. 8, No. 1, 1994, pp. 107–123. doi:10.1006/jfls.1994.1005

[18] Rai, M. M., and Chakravarthy, S. R., "An Implicit Form of the Osher Upwind Scheme," *AIAA Journal*, Vol. 24, No. 5, 1986, pp. 735–743.

[19] Schlichting, H., *Boundary Layer Theory*, McGraw–Hill, New York, 1979.

[20] Harris, C., "Two-Dimensional Aerodynamic Characteristics of the NASA 0012 Airfoil in the Langley 8-Foot Transonic Pressure Tunnel," NASA TM-81927, 1981.

[21] Coles, D., and Wadcock, A. J., "Flying Hot Wire Study of Flow Past an NACA 4412 Airfoil at Maximum Lift," *AIAA Journal*, Vol. 17, No. 4, 1979, pp. 321–328.